Local and remote atmosphere-ocean coupling during extreme warming events impacting subtidal ocean temperature in an Antarctic embayment

A. Piñones[1,2,3,4*], N. Aziares-Aguayo[5], P. Amador-Véliz[1], O. Mercado-Peña[1,3], A. González-Reyes[2,6], N. Valdivia[1,2], , J. Garcés-Vargas[1,2], I. Garrido[1,2,7,8], L. M. Pardo[1,2], J. Höfer[2,9]

[1] Instituto de Ciencias Marinas y Limnológicas, Universidad Austral de Chile, Valdivia, Chile

[2] Centro FONDAP de Investigación en Dinámica de Ecosistemas Marinos de Altas Latitudes (IDEAL), Valdivia, Chile

[3] Centro de Investigación Oceanográfica COPAS-COASTAL, Universidad de Concepcion, Chile

[4] Millenium Institute Biodiversity of Antarctic and Subantarctic Ecosystems, Chile

[5] Marine Energy Research and Innovation Center (MERIC), Santiago, Chile

[6] Instituto de Ciencias de la Tierra, Universidad Austral de Chile, Valdivia, Chile

[7] Department of Biology and Quebec-Ocean Institute, Université Laval, Québec, QC, Canada

[8] Laboratorio Costero de Recursos Acuáticos de Calfuco (LCRAC), Facultad de Ciencias, Universidad Austral de Chile, Valdivia, Chile

[9] Escuela de Ciencias del Mar, Pontificia Universidad Católica de Valparaíso, Valparaíso, Chile

Corresponding autor (*): Andrea Piñones, andrea.pinones@uach.cl

Key Points:

- Subtidal ocean temperatures (subT) in a coastal Antarctic embayment responded to extreme warming events.
- SubT recorded Marine Heat Waves (MHW) in summers 2017 and 2020, also identified as years of extreme negative SAM prior to extremely high subT
- The main dominant modes of subT variability were related to the Amundsen Sea Low (ASL) and the Southern Annular Mode (SAM)

Abstract

Coastal ocean temperatures may respond to different atmospheric and oceanic processes at local spatial scales or through remote teleconnections. In this study, the response of shallow subtidal ocean temperatures (subT, 10 m) recorded between February 2017 and January 2022 to extreme warming events during austral summer and the coupling of atmospheric and oceanic conditions was explored at a regional and local spatial scale. Temperature arrays were moored at Maxwell Bay in the northern Antarctic Peninsula (AP). Analysis for the identification of Marine Heat Waves revealed that March 2017 and January-February 2020 were the most active and extreme summers. Both years were related to extremely negative SAM index observed 3-4 months before subT increased. Analysis of the evolution of the events separately showed that in March 2017 observed temperatures were over 1ºC the climatological mean. A strengthened Amundsen Sea Low (ASL) and a blocking anticyclone moving between the Scotia Sea and the South-West Atlantic Ocean deflected westerly winds, providing and favoring the anomalous transport of warmer northern air masses to the AP. In January-February 2020, the highest subT on record was reached (2.97ºC), but air-sea heat fluxes did not show a similar pattern. In February 2020 one of the most intense atmospheric heatwaves ever recorded in Western Antarctica was observed consistent with maximum subT and positive SST anomalies that extended throughout the western region of the Southern Ocean related to extreme negative SAM. This study provided insights on the impact of strong MHWs, a topic less documented in Antarctic coastal regions.

Plain Language Summary

Understanding how ocean temperature varies and how temperature responds to different local and remote forcings is important to quantify the potential impact that temperature fluctuations may have in the coastal Antarctic environment. Between 2017 and 2022 in Maxwell Bay-Antarctic Peninsula, the response of subtidal ocean temperatures (subT, 10 m) to extreme warming events was recorded and compared to atmospheric and oceanic conditions. Extreme warming events in the ocean identified as Marine Heat Waves occurred in March 2017, January, and February 2020. During March 2017 subT exceeded by over 1ºC the historical averaged temperature. The increase in subT was related to westerly winds (usually dominate these latitudes) deflected to the south, transporting warmer northern air to the Peninsula. In January 2020, the highest subT on record was reached (2.97ºC). Observations suggested that warmer sea surface temperature was related to the

negative Southern Annular Mode (SAM) index in 2019. This study provides insights into the environmental variability and temperature ranges that affect Antarctic marine communities.

1. Introduction

Few studies have focused on understanding how atmospheric and oceanographic processes control the scales of variability of nearshore environments, fjords, and embayments of the northern Antarctic Peninsula (Chang et al., 1990; Smith et al., 1995; Schloss et al., 2012; Yoo et al., 2015; Meredith et al., 2018; Ruiz Barlett et al., 2021). The processes that dominate and control the scales of temporal and spatial variability in environmental factors frequently are described as nonlinear and are the result of dynamic interactions between the ocean and atmosphere at different temporal scales (Gill, 1982). At high latitudes such as Antarctica, continuous time series measurements of ocean characteristics are scarce due to the difficulty posed by maintaining and servicing year-round records and sampling stations. However, these records are fundamental to understanding coupled atmospheric and oceanic processes.

At the northern tip of the western Antarctic Peninsula (AP) and since January 2017, Maxwell Bay has been one of the coastal areas targeted by the Research Center Dynamics of High Latitude Marine Ecosystems (IDEAL) which has focused on understanding the impacts of environmental stressors caused by climate change on the productivity of marine ecosystems (Iriarte et al., 2019). Within Maxwell Bay, other long-term research initiatives managed by the Korean Antarctic Program at King Sejon Station (Yoo et al., 2015) and the Argentinian-German Antarctic Programs at Carlini Station (Schloss et al., 2012) have historically maintained a continuous sampling of some oceanic and atmospheric parameters inside Marion and Potter Coves respectively. Most of the studies undertaken to understand Maxwell Bay's temporal variability and dynamics have taken place during austral summer. Recently, the hydrographic variability at Maxwell Bay and its tributaries has been described by Llanillo et al. (2019). The study shows that circulation in the upper 200 m is influenced by tidal and wind forcing. In the absence of winds, tidal forcing plays a role in the variability of temperature and salinity, by contributing to the intrusion of modified Upper Circumpolar Deep Water (UCDW) from the Bransfield Strait into the bay below 70 m. Circumpolar Deep Water (CDW) is a relatively warmer, saltier and high-nutrient water mass observed below 200 m, contributes to the heat and nutrient budgets over the western AP shelf. A modified version of its upper branch (i.e. UCDW) is observed in the Bransfield Strait at 350-400 m (Sangrà et al., 2011). In the surface layer the water column of Maxwell Bay is fresher and colder, strongly influenced by meltwater from glaciers (Höfer et al., 2019). During austral summer wind

events (>6 ms^{-1}) break down summer stratification, promote mixing and contribute to organic matter advection out of the euphotic zone. In between these strong wind events, a few days of weak winds (2-3 days), enhance water column stability that sets up the conditions for massive phytoplankton blooms (Höfer et al., 2019).

In the recent decade, extreme climate events like marine heat waves (MHWs) have impacted the ocean. These events are defined as prolonged periods of persistent anomalous high temperatures over an oceanic region (Hobday et al., 2016). Their frequency and magnitude have increased in recent years as the result of anthropogenic climate change (IPCC, 2020). MHWs in the Southern Ocean have been less documented than in other regions of the world. Between 2002-2018, 19 summer MHWs were identified at a circumpolar scale, where 6 out of 19 were coastal events (Montie et al 2020), none of the events tracked was placed at the western AP and all the identified events developed during austral summer. Recently, at the northern western AP in Potter Cove - South Shetland Islands, a set of MHWs were identified from bi-weekly historical CTD samplings and MUR SSTs for January and February 2020 (Latorre et al., 2023), 2 MHWs were identified to impact water column stratification and the microbial community structure and plankton metabolism in a coastal Antarctic region. The environmental factors leading to these MHWs were not explored in the study of Latorre et al (2023), but the year 2020 particularly the summer was one of the warmest ever recorded (González-Herrero et al., 2022), these extreme events likely triggered the MHWs previously mentioned (Latorre et al., 2023) and they were probably related to long-term ocean warming (González-Herrero et al 2022).

Atmospheric processes impact the climate of western AP at various time scales. Key climate drivers include the Amundsen Sea Low (ASL), the Southern Annular Mode (SAM), and El Niño–Southern Oscillation (ENSO). The ASL, a mobile low-pressure system in the Ross Sea, the Amundsen Sea, and the Bellingshausen Sea, plays a crucial role in shaping the climate of the WAP. It influences the meridional wind patterns, affecting sea ice extent, temperature, and precipitation in the region (Turner et al., 2013; Coggins & McDonald, 2015; Clem et al., 2016; Hosking et al., 2016; Raphael et al., 2016; Goyal et al., 2021). The clockwise circulation around the ASL leads to a northerly flow, enhancing marine air intrusion and raising surface air temperatures (Hosking et al., 2013). Years with a weak ASL result in extensive sea ice and abundant precipitation, while a strong ASL leads to the opposite conditions in the western WAP (Turner el al. 1997).

The SAM is the dominant mode of atmospheric variability in the Southern Hemisphere and typically explains 35% of the extra-tropical atmospheric circulation (Hall & Visbeck, 2002; Marshall, 2007). A negative (positive) SAM phase corresponds to positive pressure anomalies in Antarctica and weakened (strengthened) westerly winds. The study by Doddridge and Marshall (2017) found that austral summers with a negative (positive) SAM preceded warmer (colder) sea surface temperatures and a reduction (expansion) in sea ice around Antarctica. SAM can also exhibit a non-annular component, particularly in the Amundsen Sea Low (ASL) region (Lefebvre et al., 2004), leading to changes in meridional winds and sea ice extent. Additionally, positive SAM trends (Thompson et al., 2000; Marshall, 2003; Arblaster & Meehl, 2006; Abraham et al., 2014) in recent decades have led to northerly and warmer meridional winds in certain areas, which can reduce (increase) sea ice and increase (decrease) sea surface temperatures (Lefebvre et al., 2004). Conversely, Schlosser et al. (2018) mention that negative SAM can result in a weakening of westerly winds and increased meridional heat exchange over the Southern Ocean.

Local and remote atmospheric variability influences and impacts the coastal ocean of the northern AP. This study aims to document extreme like events in the Antarctic coastal ocean defined as MHWs and describe the atmosphere-ocean interaction during summer MHWs at regional (WAP) and local (Maxwell Bay) spatial-scales for the northern Antarctic Peninsula, a region highly threatened by anthropogenic forcing. MHWs were identified using subtidal temperature records and OSTIA reanalysis (Donlon et al., 2012). Subsequently, dominant modes of low frequency temporal variability like SAM and ASL were explored through the analysis of sea surface temperature and atmospheric variables to find the connection with these extreme events, and lastly the atmosphere-ocean coupling on a small embayment was explored. This study contributes to the understanding of the impact of extreme events, which have not been well-documented in Antarctic coastal regions. It highlights the sensitivity of this area to climate-induced changes, as it hosts a rich and unique marine ecosystem.

2. Data and Methods

2.1 Subtidal Temperature records

Continuous coastal ocean temperature records at high latitudes such as Antarctica are scarce due to the logistical challenge of maintaining and servicing year-round sampling stations. This study analyzed temperature time series obtained at Maxwell Bay (also known as Fildes Bay), located on King George Island, part of the South Shetland Islands (SSI) at the northern tip of the AP (Fig. 1). This represents one of the many embayments located at the SSI, exposed to similar atmospheric and oceanographic forcing. From February 2017 to March 2022 (persists to this day), continuous shallow subtidal (from mean low water sea level) temperature (subT) has been registered at four points along the coastline of the bay; these sites were named as Albatros, Suffield, Artigas and Collins, being this last one the site closest to a glacier (Bellingshausen Ice Dome, Fig. 1c).

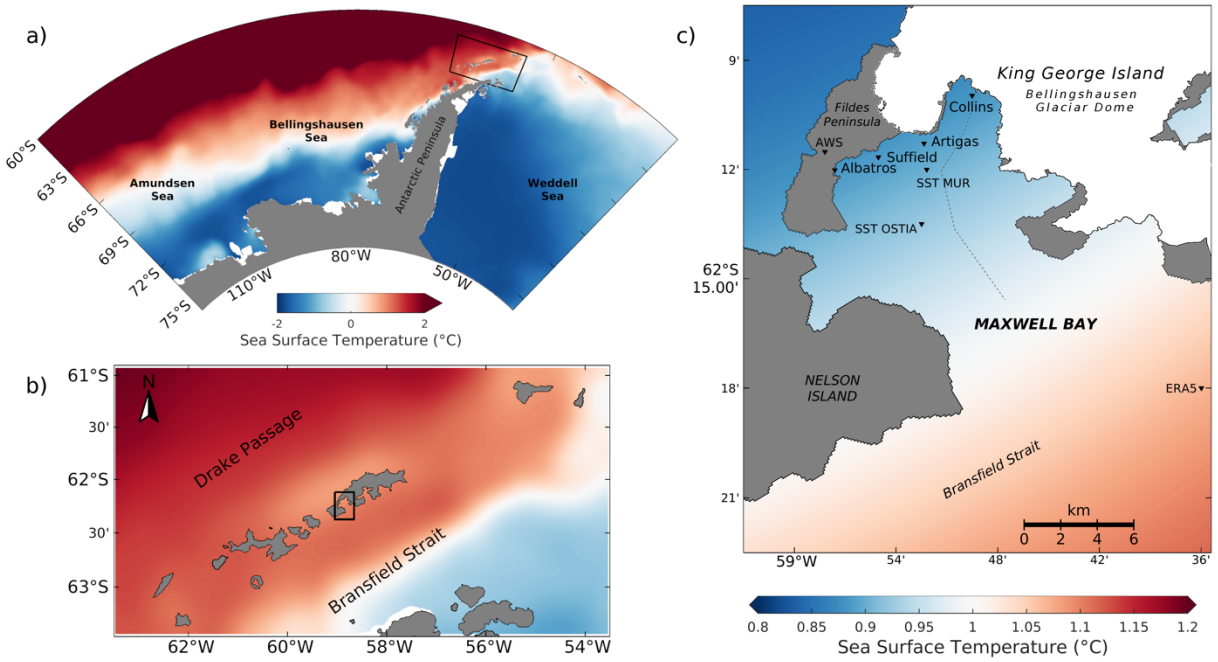

Figure 1. a) Map of the study area showing the Antarctic Peninsula and the location of the Amundsen, Bellingshausen, and Weddell Seas. The black box shows the location of the northern Antarctic Peninsula (AP). The average Austral summer Sea Surface Temperature (SST) from OSTIA reanalysis between 1982-2022 is shown in color. In b) is the location of the South Shetland Islands surrounded by the Bransfield Strait in the south (poleward) and the Drake Passage in the north (equatorward), and the location of Maxwell Bay is indicated by the black rectangle. In c) is the location of Maxwell Bay, where four study sites (black triangles) measured subtidal temperatures (subT), these were named Albatros, Suffield, Artigas and Collins, an automatic weather station (AWS) location is also indicated (inverted black triangle). The position of the

pixels used for OSTIA and MUR time series is also indicated. Segmented line indicates position of the CTD transect completed during the month of January in 2017-2020 and 2022.

At each site, a self-contained thermistor (Star-Oddi DST CT) was deployed recording temperature (±0.1 accuracy) and conductivity (±0.8 mS/cm accuracy) every 30 min. For this study, only the temperature time series were analyzed, the salinity derived from conductivity had spiked values and erratic observations that did not fulfill a quality control done to the raw data. Each sensor was encased in a PVC pipe, housed in a concrete block, and deployed by SCUBA divers at ca. 10 m depth from mean low water sea level. Since its deployment in February 2017, measurements have only been interrupted once every year for maintenance, carried out in January or February of each year. The sensors were not installed in the same site when they were removed for service, at every maintenance, they are randomly replaced at each site. Data loss occurred while servicing the CTDs, resulting in approximately 10 days of missing data for the 2018 season and 1.5 months for the 2019 season. Maintenance was done for all stations in January 2020, but Albatros was serviced and deployed a second time in mid-January after the unusually high atmospheric temperature registered during January. Due to the pandemic, since 2020 the records could not be retrieved, a situation that was normalized in 2022, when all CTDs were replaced by new ones.

Significant increases in surface ocean temperatures that lasted for a prolonged (≥ 5 days) period recognized in the literature as a MHW (Hobday et al., 2016; Oliver et al., 2021) were estimated during the study period of February 2017 to March 2022. The subT time series analyzed in this study were not long enough to allow identification of MHWs using the methodology described by Hobday et al (2016), because this method requires a 30-year record to estimate climatology. Therefore, to overcome this fact, OSTIA SSTs time series was obtained for the location closest to Maxwell Bay, the extended time series was used to estimate climatology and the 90th percentile. Prior to estimating MHWs a validation between reanalysis ocean products (ERA5-SST, MUR-SST and OSTIA-SST, see below) and *in situ* ocean temperature were done, validation is explained in the following section and additional information is provided in the supplementary. The use of reanalysis ocean products in the identification of MHWs have been used before in other regions of the world (Androulidakis & Kourafalou, 2022; Pujol et al. 2022; Li et al., 2023; Sun et al., 2023) and recently implemented for the northern AP (Latorre et al., 2023).

2.2 Atmospheric and ocean observations, validation, and climatic index

Atmospheric records were obtained from Eduardo Frei Montalva Automatic Weather Station located in Fildes Peninsula, next to Maxwell Bay (Fig. 1c). This station is maintained by the Dirección Meteorológica de Chile and data are available online at https://climatologia.meteochile.gob.cl/. Time series of hourly surface air temperature (SAT), wind direction and speed were obtained for the period January 1981 – December 2022. Wind vectors were rotated with respect to the axis of maximum variability. This was consistent with the main Maxwell Bay entrance, wind time series were presented as vectors from (toward) the Brasfield Strait or toward (away) the sampling sites (subT sites), that corresponded to winds mainly from the southeast (northwest). Rotated wind was only used in the comparisons of subT, SAT and heat fluxes terms.

ERA5 reanalysis data from the European Centre for Medium-Range Weather Forecasts (ECMWF) was used to analyze atmospheric conditions. The data has a horizontal resolution of 0.25 x 0.25 degrees. In addition, Mean Sea Level Pressure (MSLP), 2 m air temperature (hereafter surface air temperature), and vertical integral of northward heat flux (hereafter meridional heat flux) were used to investigate anomalous warm air flux into the study region. Hourly heat flux terms (sensible, latent, shortwave and longwave radiation) were obtained from ERA 5 between January 2017 and December 2022 and the total net heat at the ocean surface was estimated to show heat gain (positive values) or loss (negative values) from the ocean.

Daily SST for anomaly fields and the marine heat waves analysis (see below) were obtained from the Operational Sea Surface Temperature and Ice Analysis-OSTIA (Donlon et al., 2012). The data is available at the website https://catalogue.ceda.ac.uk/uuid/62c0f97b1eac4e0197a674870afe1ee6. This product has a spatial grid resolution of 0.05º (Reynolds et al., 2007) and covers the period 1982 onwards. Daily sea surface temperature (SST) data between June 2002 until December 2022 was obtained from the Multi-scale Ultra-high Resolution (MUR) Analysis managed by the Environmental Research Division's Data Access Program (ERDDAP). MUR SST data has a spatial resolution of 0.01°. The locations of the OSTIA and MUR SSTs pixels used for the analysis are depicted in Fig. 1.

Visual and statistical comparisons were done between *in situ* observations (surface and 10 m CTD data) and reanalysis SST products (see Fig. 2, S1-S2). A Taylor diagram analysis (Fig. S1) was completed to correlate the average subT time series with OSTIA and MUR SSTs. Higher correlations were obtained between subT and OSTIA SST, therefore, this last data product was used for all other consecutive analysis (more information is provided in the next section). OSTIA SST anomaly Hövmoller was calculated for the 1982-2015 monthly climatology over the complete West Antarctica region, averaged from 60ºS to 65ºS. Other anomalies in this study were also calculated for the 1982–2015 monthly climatology over the region 125ºW – 50ºW, 50ºS – 76ºS, including the Amundsen Sea (125ºW – 100ºW), Bellingshausen Sea (100ºW – 60ºW), the AP and western Weddell Sea (60ºW – 50ºW) (Fig. Fig.1a).

SAM index was obtained from https://legacy.bas.ac.uk/met/gjma/sam.html. This index is calculated from observed MSLP differences between stations located in Antarctica and at midlatitudes (Marshall, 2003). To calculate the ASL's strength and position, the ASL indices from Hoskin et al. (2006) were used. These include the ASL Actual Central Pressure Index which defines the ASL strength as the minimum MSLP value in the ASL sector, consistent with the method used by Turner et al. (2013), and the ASL latitude and longitude which is the position of the ASL. These indices were calculated using monthly ERA5 MSLP data for the area 62ºW–190ºW, 60ºS – 80ºS.

2. 3 Identification of Marine Heat Waves and comparison of *in situ* subT with reanalysis ocean products

Climatologies for the period 1982-2015 were used to compare the strength and position of the studied events. To determine how subT compared with climatological ocean temperature from the last 30 years, an analysis following the determination of marine heat waves was implemented using the methodology of Hobday et al. (2016). This defines MHWs as continuous events of warm SST anomalies exceeding a threshold (90th percentile with respect to a 30-years climatology) during at least 5 days. This methodology was applied to the OSTIA-SST reanalysis using a moving baseline climatology (Roselló et al., 2023). To identify the summers with higher number of MHWs events per year and to provide an assessment of the duration and strength of MHWs during the subT records 2017-2022.

OSTIA-SST reanalysis was selected over MUR-SST reanalysis because the visual and statistical correlation with *in situ* subT time series was higher. Seasonal trend decomposition using LOESS (STL) was implemented to estimate and remove seasonal variability (Cleveland et al., 1990). This analysis is a filtering tool that decomposes time series in seasonal, trend and remainder components (residuals). To estimate the relationship between subT and OSTIA-SST, a correlation was performed between both data sets and after removing trend and seasonal variability the residuals were compared (Fig. S2). The relationship between *in situ* subT and OSTIA-SST was linear and both data sets provided a correlation of 0.97 (Fig. S3). The correlation of the residuals presented a dispersion concentrated around the intercept (0.0) and was homogeneous around this point, which indicates that both data sets are highly related and the biases that can be obtained in the identification of marine heat waves and other temperature changing processes may have a lower error. The small difference observed during fall-early winter cooling periods could be attributed to the difference in the spatial resolution of two different ocean products (*in situ* versus reanalysis). However, during the spring and summer periods from 2017 to 2021 (ocean heat gain) both ocean products were in phase and consistently represented the same temporal variability. Identification of MHWs using OSTIA-SST has been done in other regions of the world like the Java Sea, southern Europe-Western Asia and eastern boundary current systems (Iskandar et al., 2021, Bonino et al., 2022, Song et al., 2023) has proved to be a reliable reanalysis product for the identification of synoptical changes such as MHWs and marine cold spells (Peal et al., 2022), thus the data assimilation scheme used by OSTIA is continuously update it (Good et al., 2020).

3. Results

3. 1 Identification of MHWs in subT time series and OSTIA-SST

Subtidal temperature (subT) records and OSTIA SST showed a marked annual cycle, the four sites of subT showed a unified behavior of the system inside Maxwell Bay. Temporal variability of the four-time series was very similar (Pearson's correlation of r=0.99) (see Fig. 2 and Table 1). SubT time series were compared to ocean temperature at depth from in situ CTD observations (see Fig. S4 summer cruises performed between 2017-2022, Fig. S5). From surface to approximately 7-15 m, subT showed that is representing the summer variability of the upper water column. Additional comparisons were done between OSTIA and MUR SSTs (Fig. S1). Higher correlation was obtained between subT and OSTIA SST (Fig. S1).

Table 1. Overall statistics of subtidal temperatures in ºC. SD is standard deviation, Min and Max are the minimum and maximum temperatures respectively.

Station	Mean	SD	Mean Dec-Feb	Mean Jul-Sep	Min	Max
Collins	-0.27	1.17	0.97	-1.61	-1.98	2.22
Artigas	-0.36	1.13	0.86	-1.60	-1.92	2.44
Suffield	-0.42	1.13	0.84	-1.64	-1.94	1.97
Albatros	-0.26	1.14	1.03	-1.49	-1.90	2.97

The average subT at Maxwell Bay was -0.33ºC, and during the winter months (July-September) the average subT was -1.58ºC, with a minimum of -1.98ºC recorded at Collins station, right next to the site closest to the glacier; the averaged of the four subT records during austral summer was 0.92ºC. Estimation of MHWs for the study period showed that in March 2017 a significant increase in subT was observed, which was not measured in other early autumns of the time series. The time series of OSTIA showed a first increase that peaked at the end of February while the second peaked by the end of March, these events were detected as MHWs (Table 2) but are not highlighted (in red) in Fig. 2 because *in situ* observations (subT) started recording after the heatwave begun. During March 2017 subT reached over 1ºC and persistently continued until mid-April consistent with the identification of the MHW category II-strong identified with OSTIA (Table 2). No other April started with a temperature higher than 1.51ºC like the one recorded for April 1, 2017. Thus, subT records during March were 0.9ºC above the historic (30 years) 90th percentile time series temperature (Fig. 2). According to the analysis of Hobday et al. (2016) for MHWs, the anomalously higher temperature registered in March would fit the definition of a strong warming event (Table 2). For the rest of the time series, the number of days above the 90th percentile was higher primarily during fall-winter seasons consistent with a study that previously described warmer winters in the Antarctic Peninsula (Sato et al., 2021). Significant subT decreases were observed in April, reaching values close to 0ºC in only a few days. Specifically, the most drastic temperature drop was recorded in mid-April at the Albatros station with a rate of temperature decrease of 0.07 ºC hour^{-1}. The summer season that presented the highest subT of the record was observed in January 2020, where the maximum subT registered was 2.44ºC and 2.97ºC in the Artigas and Albatros stations respectively. The time series of subT showed values of 1.1ºC above the historical 90th percentile (Fig. 2).

Table 2. Category II – strong Marine Heat Waves (MHWs) identified at the Maxwell Bay, using methodology proposed by Hobday et al. (2016). Max intensity corresponds to the highest temperature anomaly value during a MHW.

Event name	Date range	Peak date	Category	Max intensity (ºC)	Duration (days)
Event 2017 January	2017-01-30 / 2017-03-01	2017-02-13	II Strong	0.98	31
Event 2017 March	2017-03-16 / 2017-04-07	2017-03-28	II Strong	0.92	23
Event 2020 January	2020-01-04 / 2020-01-29	2020-01-20	II Strong	0.73	26
Event 2020 February	2020-02-03 / 2020-02-20	2020-02-09	II Strong	0.95	18

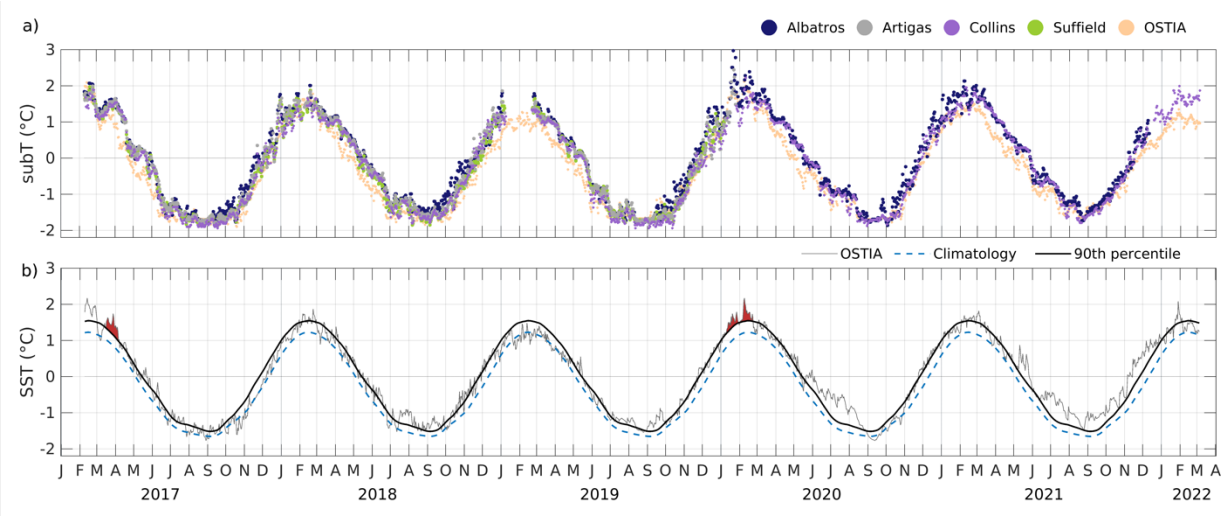

Figure 2. In the upper panel. Time series of daily subT (ºC) recorded with DST for the stations Albatros (blue), Suffield (green), Artigas (grey) and Collins (violet) at Maxwell Bay. In the lower panel. Daily OSTIA-SST time series closest to Maxwell Bay. The estimated historic (last 30 years) 90th percentile and climatology of ocean temperature are shown by the black line and blue dash line respectively.

The regional representation of SSTs and identification of extreme ocean warming events within the November and March season between the years of subT records showed a consistent increase in the number of MHWs for 2017 and 2020 (Fig. 3). This was consistent with the events of anomalous high subT registered in March 2017 and January-February 2020. In 2017 a large area along the western AP presented around 15-20 MHWs, and the region around the South Shetland

Island presented between 10-15 of MHWs between November and March. During 2020, a year identified as one of the most active years in terms of atmospheric heat waves, presented a large area along the western AP and northwest towards the Bellingshausen Sea, with events between 15-20 between November and March. Around the SSI the same number of events was observed as during 2017 (10-15 events/5 months). During, 2018, 2019, 2021 and 2022 and particularly around the SSI, there was no evident observation of MHWs at the same rate as 2017 and 2020. However, after 2020 the area east of AP, towards the western Weddell Sea, appears as a region where marine heat wave activity was increasing (higher than 10-15 events/5 months). These results indicate that warming of the Bay was not a localized response of ocean temperature but rather it is synchronized to a regional warming.

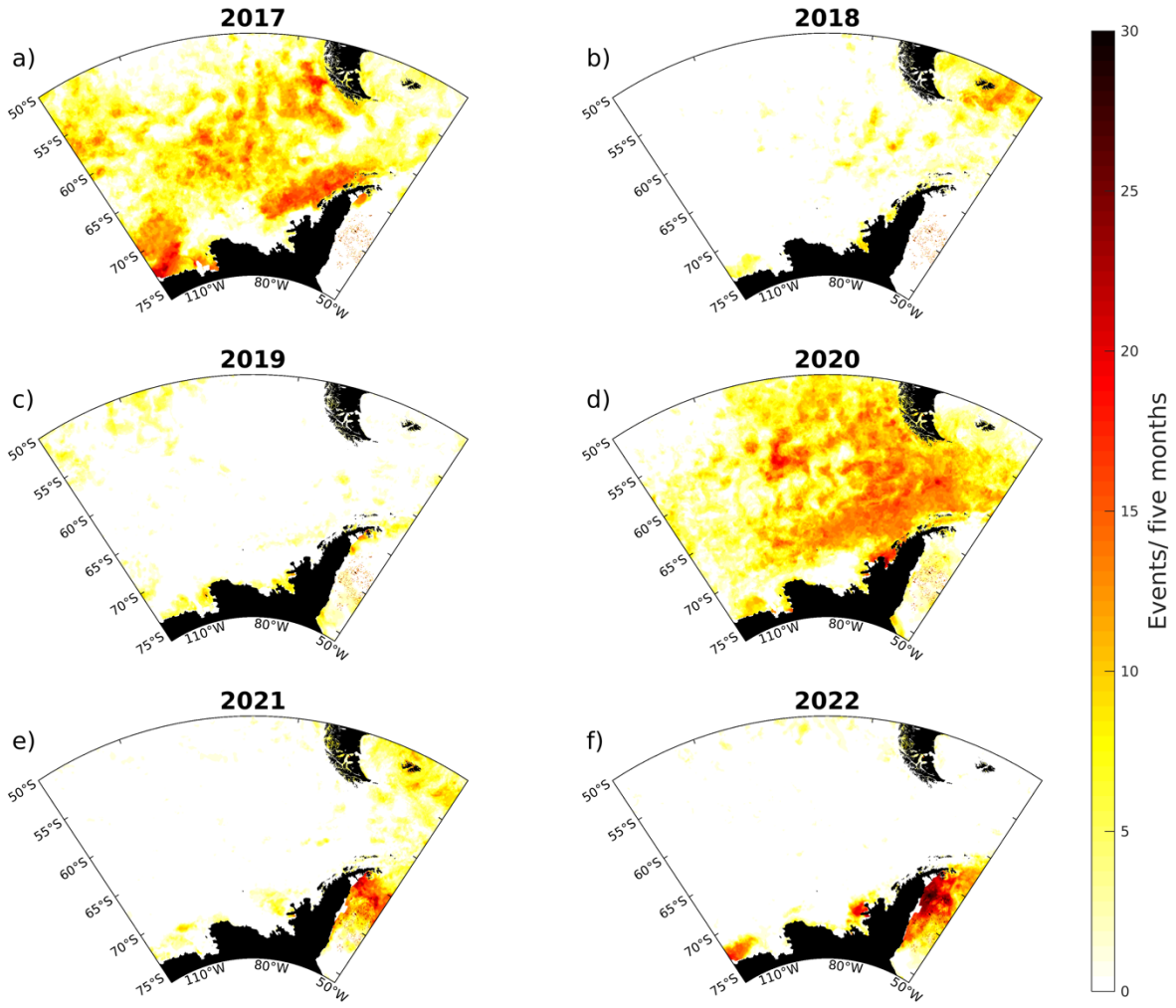

Figure 3. Number of Marine Heat Waves (MHWs) recorded during the months of November to March for the years 2017-2022 following the methodology described by Hobday et al. (2016).

3.2 Regional Sea Surface Temperature Anomalies and SAM index

For a better understanding of larger spatial scale processes involved in the anomalies found in subT records and the linkages with regional scale processes, a Hövmoller diagram for SST (Fig. 4) was made for the Western region of the Southern Ocean between January 2016 and February 2022. The presence of a SSTa dipole generated by El Niño 2015-2016 mentioned by Stuecker et al. (2017) was observed between 125º and 90ºW. Maxwell Bay was (vertical dashed line) located in the negative sector of the dipole and the positive signal of the dipole did not impact the study area. This suggests that the SSTa dipole related to El Niño did not generate subT increases at Maxwell Bay.

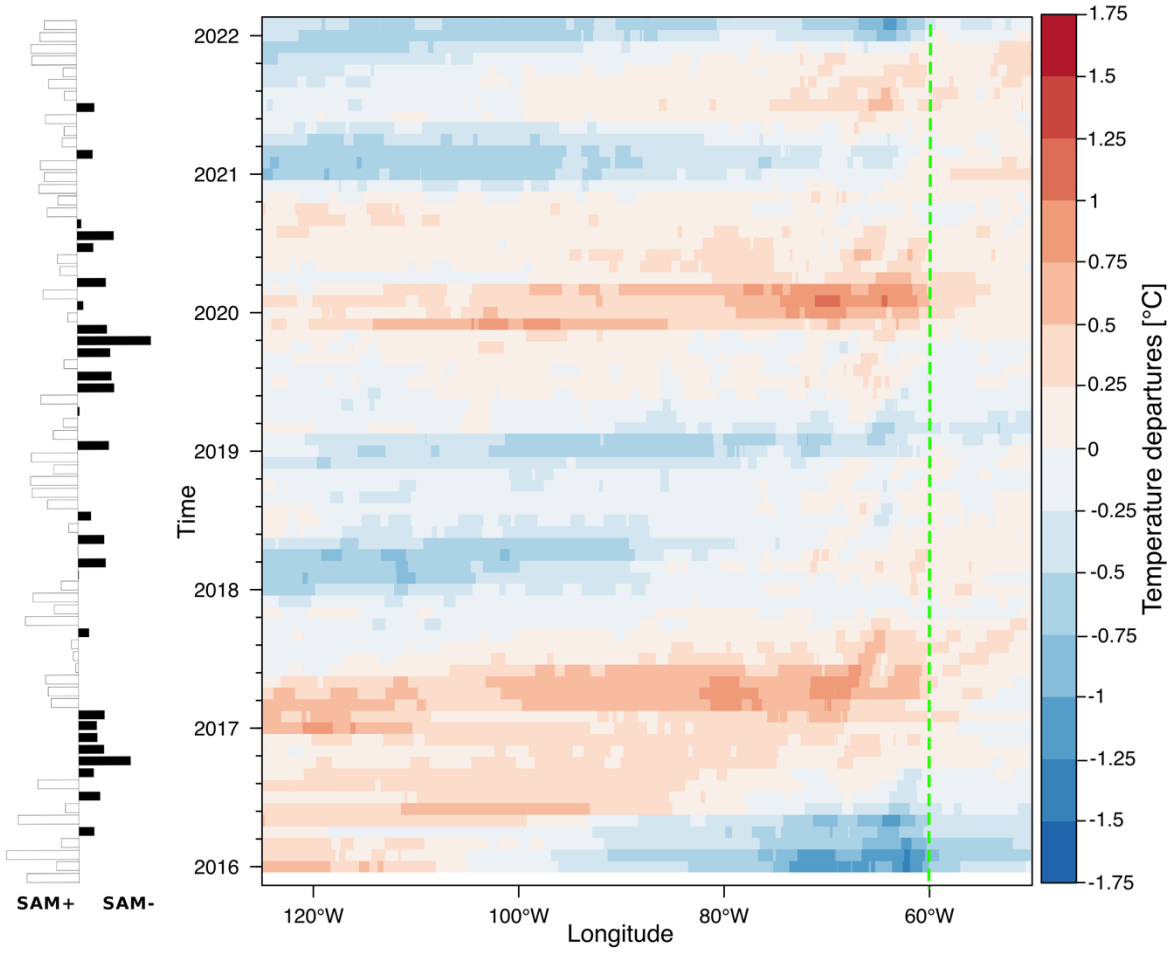

Figure 4. Hövmoller diagram (right side) for the temporal evolution of SST anomalies (ºC) at the Western region of the Southern Ocean (averaged from 60ºS to 65ºS). Anomalies were calculated

with respect to the climatological monthly mean from the period 1982 to 2015. Maxwell Bay location is shown with a green dashed line. On the left, the monthly mean SAM index is shown, where positive values are in white and negative values are in black.

Two bands of positive SST anomalies extended throughout the Western region of the Southern Ocean, these were observed during both periods corresponding to October 2016-March 2017 and October-December 2019, which corresponded to extremely negative SAM events reaching larger positive anomalies in late 2016 and 2019 (Fig. 4 left, Doddridge & Marshall, 2017). In March 2017 these positive anomalies remained, consistent with increases in subT in the bay, that reached 0.5°C but being lower than other sectors around (Fig. 4, right). In January 2020 SAM index turned positive, but it is well established that the influence of SAM on SST can be observed during the following months (Doddridge & Marshall, 2017). In this month the highest anomaly for the bay was observed (1.16ºC obtained with the average of the two points closest to the bay; Fig. 4 right). This may suggest that positive SST anomalies that were SAM related, could be associated to the subT increases observed during January-February 2020 in the bay and consistent with the months of higher activity of MHWs.

3.3 Atmosphere-ocean exchange of heat along the Bellingshausen Sea region during three MHWs

The high subT recorded during later summer of 2017 could be related to atmospheric weather patterns that favored northernly warm air advection and maintained a high-pressure system on the northeastern AP (Fig. 5a). The maximum annual air temperature was reached in March as the wind blew from the W-N for half the month. This was caused by the intensification of the ASL and the presence of a blocking anticyclone that prevailed in March between the Scotia Sea and the South-West Atlantic Ocean, generating a MSLP anomaly dipole on the Amundsen-Bellingshausen Seas (ABS) (Blunden et al. 2018) as shown in Figure 5a.

The ASL extended throughout the ABS and reached a minimum sea level pressure at its central point of 975.1 hPa, which was deeper than the climatological average but within normal ranges. Furthermore, the location of the ASL for March was found further north (66.25ºS) than the climatological position (68.7 ºS) for March and even further north than the northernmost point of its climatological annual latitudinal range (66.35º ± 4ºS). Moreover, the anticyclone with high

MSLP anomalies that exceeded 20 hPa in some sector caused blocking of the westerly winds, diverting them to the Peninsula, triggering an unusual and intense northernly meridional heat flux, advecting positive surface air temperature anomalies from the northwest of the AP to near the coast of the Amundsen Sea (Fig. 5d and 5g). In April, the MSLP dipole was still present but weaker and displaced further west, causing southern flow (low surface air temperature) to move over the AP. It is worth mentioning that, in November 2016 the SAM index reached a historical November negative record (the third in the satellite era), and during early 2017, the SAM index continued to be negative.

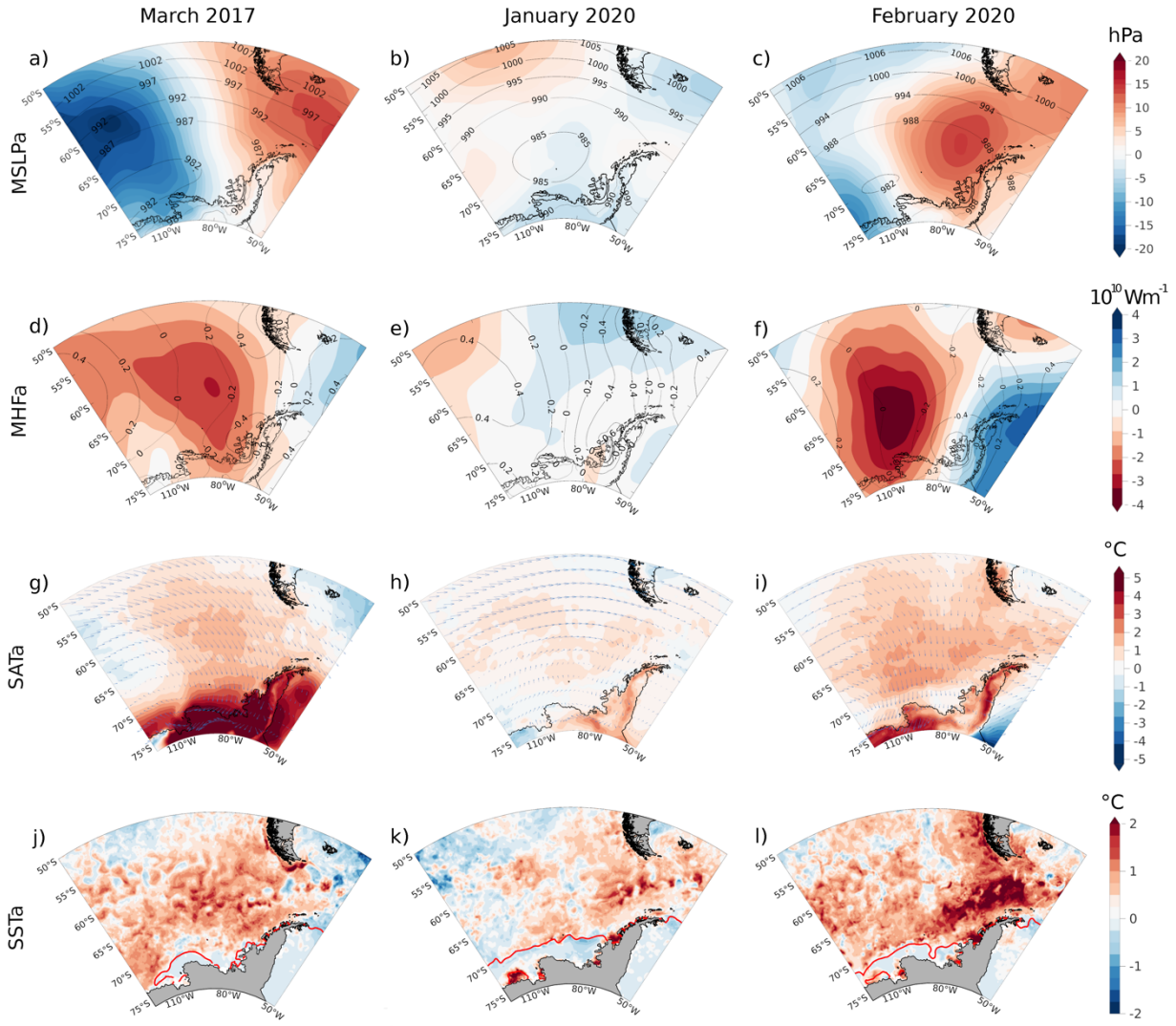

Figure 5. Atmospheric and oceanic conditions for the periods March 16 – April 7, 2017 (left column), January 4-29, 2020 (mid-column) and February 3-20, 2020 (right column). The colors show anomalies, and the contours show average over time for: (a-c) sea level pressure in hPa, (d-

f) MHF, meridional heat fluxes (negative southward, in red) in 1010 Wm−1, (g-i) SAT, surface air temperature in ◦C, and (j-l) SST, sea surface temperature. Anomalies were calculated with respect to the climatological monthly mean from the period 1982-2015. Monthly mean wind vectors are shown in blue in (g-i). Red line in (j-l) shows the monthly mean ice edge.

In January-February 2020 the ASL was weakened and centered in the Bellingshausen Sea (further east than the climatological location; Fig. 5b, c). Positive meridional heat flux anomalies over the AP and air temperature anomalies of 0.8ºC (1.5ºC) in the Maxwell Bay were observed during January (February), suggesting a northernly warm air advection (Fig. 5e, f). Moreover, SSTa were positive and higher anomalies of 0.5-2ºC were observed around the SSI (Fig. 5k, l). But, in contrast to what was observed in March 2017, the strength of the ASL (Fig. 5b, c) was weaker in January-February 2020, meridional heat flux anomalies were confined to the polar and the western Bellingshausen Sea region (Fig. 5e, f) and the most noticeable presence of westerlies (Fig. 5g) were restricted to farther north in January 2020, suggesting a rather small to negligible influence of warmer air entering from the north. However, during February 2020 westerlies and 1-2ºC positive SATa were observed around Maxwell Bay and most of the western AP. Thus, SSTa were positive and higher anomalies of 1-1.5ºC were observed around the SSI (Fig. 5l). During January 2020, surface ocean warming started from the coast to the offshore region and was consistent along the western AP with the monthly mean ice edge (Fig. 5k).

3.4 Air-sea exchange at Maxwell Bay during three MHWs

Daily winds rotated to the main Maxwell Bay axis (~100º) and net heat exchange were analyzed during three MHWs (Fig. 6), it was found that during both years (gray shaded periods) net heat gain to the ocean was dominant (Fig. 6, S6). During these periods a slight decrease in the intensity of northerly winds was observed but direction remained from the north-northeast. This pattern was consistent with the regional predominance of northwesterly winds observed in Fig. 5g, and the advection of positive surface air temperature anomalies from the northwest of the AP to near the coast of the Amundsen Sea (Fig. 5d and 5g).

Between March and mid-April 2017 heat losses from the sea were almost non-existent. Figure 6 shows a net heat flux (Q_{net}) that remained positive from early March to the first days of April, subT

was above 1ºC. The days prior to the MHW, atmospheric temperature consistently increase from -5ºC to almost 4ºC and remained above 0ºC until the first days of April. Lagged correlations between March SAT and subT showed significant and positive correlations with SAT leading by 2-3 days, even after removing trends and seasonal signals to the time series, 1-day lagged cross-correlations were positive and significant at the 95% confidence level (Fig. S7). During most of the duration of the March 2017 MHW (gray shaded days) northwesterly (towards Bransfield Strait) wind was observed, during the end of the event a reduction and a change to southerly winds was observed. After the MHWs on April 21st winds changed toward the Bay (> 18 ms^{-1}), during these days SATa dropped and in general, heat flux losses were consistent with lower SAT and winds from the E and SE.

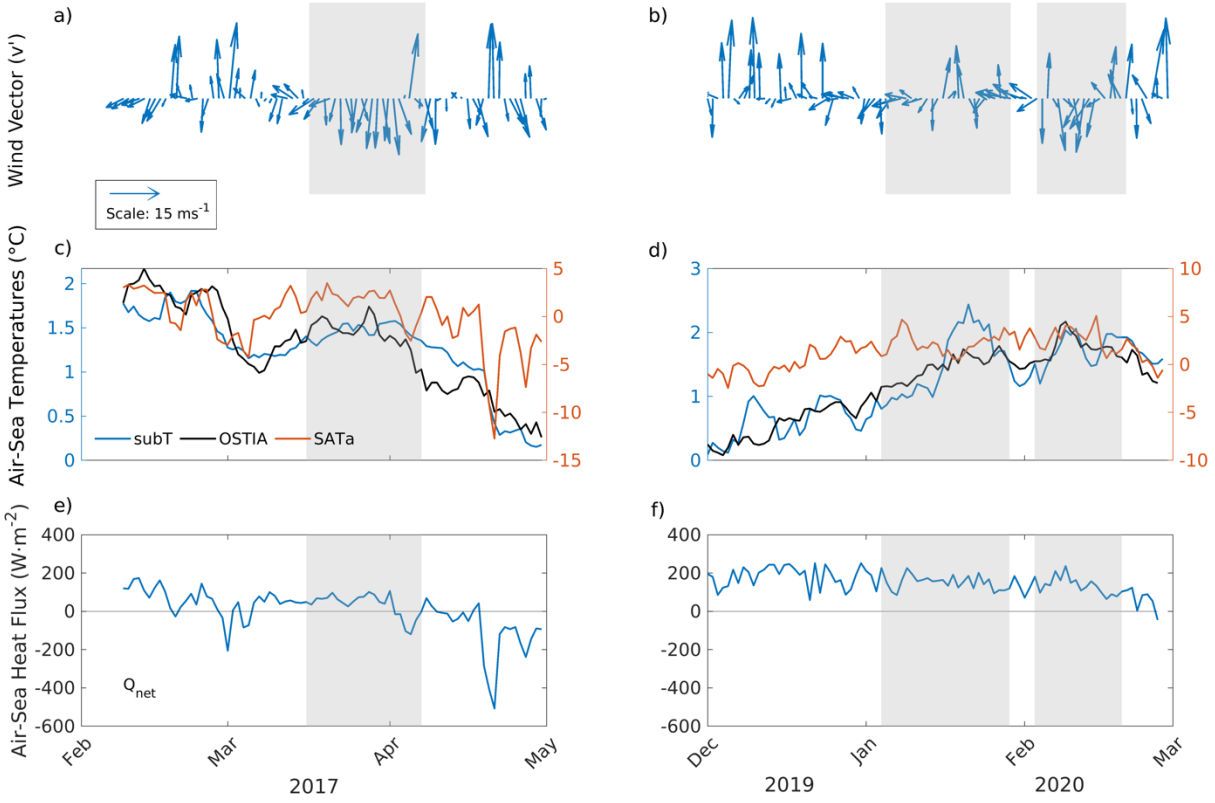

Figure 6. Time series of daily wind rotated along the main axis of Maxwell Bay (a, b), arrows pointing upward (downward) represent winds from (toward) the Bransfield Strait, *in situ* subT and surface air temperatures anomalies - SATa (c, d) and total air-sea heat flux-Q_{net} (e, f) for the three summer MHWs events identified during 2017 (left column) and 2020 (right column). Light grey areas show the extension of the three MHWs obtained from Hobday et al. (2016) analysis. Note that the scales for 2017 and 2020 for SAT and ocean temperatures were different.

The shortwave was the dominant term in the heat budget during the summer 2020 event due to that the maximum solar radiation of the year is received during this season (Fig. S6). Latent and sensible heat losses not greater than 100 Wm^{-2} were observed (Fig. S6), but these were not enough to drop the net heat flux below zero.

The highest Maxwell Bay subT of all years recorded was observed on 21 January at Albatros Station (2.97ºC). Consistent with the peak of the MHW identified during January 2020. Weak winds that on average did not exceed 5 ms^{-1} during the previous week and daily mean air temperature of 1.9ºC were recorded. OSTIA-SST slightly differed from *in situ* subT during the evolution of the January 2020 MHW. SubT records showed that the January 2020 MHW was stronger than the identified by OSTIA-SST analysis. However, other ocean temperature records inside Maxwell Bay (Latorre et al., 2023) showed that between January 15 and 23 maximum surface water column was observed exceeding 2ºC, consistent with the values registered by subT. During summer 2017 and 2020 it was possible to notice the relationship (present in almost all cases) between winds from the Bransfield Strait (E-SE band) and drops of SAT (Fig. 6). Decrease in SAT were consistent with negative relative minimum latent and sensible heat fluxes (Fig. S6) larger than -50 Wm^{-2} (except the last one on January 18). The most important heat loss event in 2017 was registered on April 20, days after the MHW ends. On this occasion, a rapid drop in subT is observed in the Albatros station, dropping below 0ºC for the first time in the year, concurrently easterly winds were registered, reaching over 24 ms^{-1} at Frei Station.

4. Discussion

4.1 Antarctic subtidal temperature response to low-frequency forcing and extreme temperature events

During the sampling period (2016-2022), extreme negative SAM events were observed (October 2016 to March 2017 and October to December 2019), with two out of the three most negative Novembers on record since the satellite era, -3.12 in 2016 and -4.42 in 2019 (see Fig. 4). Thus, these events occurred in a period in which the SAM index had been showing a positive trend during

the last decades (Thompson et al., 2000 Marshall, 2003; Arblaster & Meehl, 2006; Abram et al., 2014).

Oceanic conditions showed that during these negative SAM events positive SSTa were observed in the region between 60ºS and 65ºS (i.e. part of Drake passage and the western Antarctic Peninsula) and extended throughout the Western region of the Southern Ocean, being consistent with previous studies that related Ekman transport to negative SAM index and with positive SSTa (Doddridge & Marshall, 2017). SSTa were higher along the western AP, where coastal ocean temperature rises compared to other regions, like subT records at South Bay (64.88ºS, Doumer Island) located farther south from Maxwell Bay, showed that surface ocean heat gain was observed along the inner shelf. Ocean temperature measured at 10 and 20 m increased to 3ºC in February 2017, while during the previous summer, the highest ocean temperature recorded was 1.3ºC (Cárdenas et al., 2018).

In February 2017, the Antarctic daily sea ice extent reached one of the lowest values since the satellite era, consecutively surpassed by the February 2022 and 2023 sea ice extent (The Copernicus Climate Change Service, 2023). A 40-year record of sea ice extent showed that since 2016, yearly average sea ice has been declining (Parkinson, 2019). This marked a turnaround in the mild but positive trends that Antarctic ice has shown. Therefore, the positive SSTa are expected to be related to ice decline. However, the sea ice concentration (SIC) anomalies have shown an overall negative behavior until present (Parkinson, 2019), the positive SSTa of the band between 60º and 65ºS across West Antarctica is only observable during negative SAM events. A recent analysis of air temperature time series (since the 1950s) from weather stations in the Antarctic Peninsula showed that the mid 2010s marked the end of a warming pause consistent with the variability of SAM (Carrasco et la., 2021). This study also stated that further research is needed to assess warming trends of atmospheric temperatures on the Antarctic Peninsula.

A special interest has developed in recent years in the study and understanding of the mechanisms behind the occurrence of extreme weather events like the ones registered in 2017 and 2020 (Siegert et al., 2023). A recent analysis by González-Herrero et al. (2022) of an extreme warming event of the atmosphere in February 2020 did not find convincing evidence of the role of SAM driving the warming event, instead, they stated that if any the SAM trend had an opposite effect of climate change by weakening the warming events. However, the mechanism behind the coupling of SAM

and atmospheric heat waves should not necessarily be like the mechanism between SAM and MHWs. Another study looking at the relationship between MHWs and climate modes at a global scale found that there is a band around the Southern Ocean where negative SAM is significantly correlated with the occurrence of marine heat waves (Holbrook et al., 2019). The area was located farther upstream from the western AP, between 0-50ºE and between 80 and 130 ºE both regions along the 60ºS band. The globally analysis correlated SAM (and other climate modes) on-phase with MHWs. In our study, the significant relationship encountered between negative SAM and SSTa (Fig. 4) was observed 3 months out of phase with the SSTa lagging the record-negative SAM index.

4.2 Atmosphere to ocean heat contribution during the three warming events

A simple estimation of total heat content was obtained in subT records to further explore the potential heat sources during the MHWs in 2017 and 2020. In either case, both, the atmosphere, and the ocean showed significant and positive anomalies along the western AP (positive SATa and SSTa respectively in Fig. 5). Was SubT higher in Maxwell Bay as the result of an ocean-atmosphere heat transfer (March 2017) or was this heat advected by ocean currents into the coastal embayment of Maxwell Bay (January 2020 case) (Llanillo et al., 2019)?. The heat flux (including advective and air-sea fluxes) needed to increase the water column temperature during a time Δt was estimated using the relation $Q = \Delta H/\Delta t$, where ΔH is the change of heat contained in the volume per unit time. The Maxwell Bay ocean temperature distributions measured by Hofer et al. (2019) and the Costa et al., (2008) methodology, were used to estimate the heat required to get the observed subT. These calculations estimated that for March 2017, the heat provided by the atmosphere (Qnet) was enough to raise ocean temperature to the values observed in subT records. For January 2020, the maximum daily subT showed a significant heat difference (~125 Wm^{-2}), suggesting that an advection of heat via ocean currents is necessary. The advection of warmer water could result from observed positive SSTa likely related to SAM negative phase as already mentioned (Fig. 4 and Fig. 5k, l).

4.3 Antarctic subtidal temperature response to local forcing

559 Maxwell Bay subT responded to atmospheric and oceanic conditions during March 2017 and
560 January-February 2020. March 2017 showed the highest subT during the recorded period, not
561 reached in the other early autumns, with subT over 1ºC observed until mid-April 2017 (Fig. 2).
562 Both a strengthened ASL and the presence of an anticyclone moving between Scotia Sea and
563 South-West Atlantic Ocean deflected westerly winds (Hosking et al., 2016) and transported
564 warmer northern air toward the AP, a high-pressure system favored incoming shortwave radiation
565 and net sensible heat flux between the atmosphere and the ocean consequently increasing subT.
566
567 During January 2020, the highest subT on record was 2.97ºC, consistent with a summer of
568 unprecedented atmospheric heat waves (Robinson et al., 2020). Contrary, air-sea heat fluxes did
569 not show special gains that could indicate the influence of atmospheric forcing in the increased
570 subT. On the other hand, the highest SST anomaly for the bay was 1.16ºC, associated with
571 anomalies that extended throughout the Western region of the Southern Ocean related with the
572 extremely negative SAM index reached in 2019. Despite the positive SAM observed during
573 January 2020, the effect of SST anomalies related to negative SAM events across the Southern
574 Ocean persisted until three months after (Doddridge & Marshall, 2017). SubT records registered
575 an extended high temperature the rest of the summer and fall of 2020, around 0.3ºC above the
576 historical 90% percentile.
577
578 **5. Concluding remarks**
579
580 A unique set of subtidal ocean temperature (subT) observations were recorded since February
581 2017, providing valuable information on coastal ocean variability and the atmosphere-ocean
582 coupling effects over the nearshore environment of the northern AP. SubT records at 10 m depth
583 along Maxwell Bay showed a marked annual cycle and a unified high-frequency variability of the
584 system inside the Bay, consistent with the variability at a regional scale and other ocean
585 temperature products (i.e. ERA 5, OSTIA and MUR SSTs).
586
587 This study highlights the impact of extreme temperature events and underlines the importance of
588 large-scale and local forcing in modulating ocean temperatures. Although more studies are needed
589 to assess the impact of large-scale variability in Maxwell Bay and other similar embayments

around the northern Antarctic Peninsula, the results suggest that climatic variability and extreme events like MHWs, as well as the modes like the negative SAM phase may likely trigger the increase in coastal subtidal temperatures at the northern AP, due to positive SSTa. Similarly, the presence of a low-pressure center together with a slow-moving anticyclone in the study area triggers sea temperature increases due to the entry of northern warm airflow over AP.

Moreover, longer time series at coastal regions along the northern AP are needed to assess air-sea exchange. Further understanding of the atmospheric forcing influencing the blocking anticyclone and the ASL is needed to assess if these changes are related to other atmospheric controls, like the SAM. For instance, the Zonal Wave 3 (a distinctive feature of the Southern Hemisphere extratropical atmospheric circulation) has been related to the increase in meridional fluxes in the Southern Ocean (Raphael, 2004; Schlosser et al., 2018), and climate model projections have suggested an increase in warmer northerly winds toward the AP associated to an eastward shift of the ASL (Hosking et al. 2016) and a deepening of the ASL over the twenty-first century in response to greenhouse gas emissions (Raphael et al., 2016). The impact of marine and atmospheric heat waves influences the ocean heat balance in coastal Antarctic regions, these extreme events are projected to occur at a higher frequency as we move to the end of the century. Understanding the plausible triggering and feedback mechanisms is crucial to understanding the impact of environmental stressors on the Antarctic coastal ecosystem.

Acknowledgments

This study was funded by ANID-FONDECYT 1210988, FONDAP 15150003, Millenium Institute BASE ICN2021-002, COPAS-COASTAL ANID-PIA FB210021 and CoastCarb H2020-MSCA-RISE-2019. AP is a member of the POGO-Coastal Marine Heatwave Interdisciplinary Research group (CMHIR). NV was supported by ANID-FONDECYT grant 1230286. We thank the support provided by the IDEAL diving team (Paulina Brüning, María José Díaz, Hans Bartsch, Mateo Cáceres, and Bastián Garrido) as well as the logistical support provided by INACH. AGR thanks ANID-FONDECYT 11230437. JH thanks ANID-FONDECYT grant 1211338. We thank Dirección Meteorológica de Chile for providing in-situ atmospheric records, ECMWF for providing ERA5 reanalysis, Hosking et al. (2016) for providing ASL indices, Marshall (2020) for providing SAM index. We acknowledge Pawlowicz (2020) for the development of package

M_Map for MATLAB. This study has been conducted using E.U. Copernicus Marine Service Information. Subtidal ocean temperatures will be available in the Critterbase data platform (https://critterbase.awi.de/) and Polar Data Catalogue repository (https://www.polardata.ca/), for review purposes the subT time series were submitted as Supporting Information. All other data used in this study are available to the public as written in the text. We acknowledge the contribution of two anonymous reviewers and the Editor Dr. Laurence Padman in an early version of this manuscript. We thank Editor Dr. Anna Whålin for positive feedback and great suggestions.

References

Abram, N. J., Mulvaney, R., Vimeux, F., Phipps, S. J., Turner, J., & England, M. H. (2014). Evolution of the Southern Annular Mode during the past millennium. Nature Climate Change, 4 (7), 564–569. doi: 10.1038/nclimate2235593

Androulidakis, Y.S.; Kourafalou, V. (2022). Marine Heat Waves over Natural and Urban Coastal Environments of South Florida. Water 14, 3840. https://doi.org/ 10.3390/w14233840

Arblaster, J. M., & Meehl, G. A. (2006). Contributions of External Forcings to SouthernAnnular Mode Trends (Tech. Rep.). Retrieved from http://www.nerc-bas.ac.uk/icd/gjma/sam.htmlBlunden, J., Arndt, D. S., & Hartfield, G. (2018, 8). State of the climate in 2017 (Vol. 99;Tech. Rep. No. 8). doi: 10.1175/2018bamsstateoftheclimate.1

Bonino, G., Masina, S., Galimberti, G., & Moretti, M.- (2022). Southern Europe and Western Asia Marine Heat Waves (SEWA-MHWs): a dataset based on macro events. Earth System Science Data. https://doi.org/10.5194/essd-2022-343

Cárdenas, C. A., González-Aravena, M., & Santibañez, P. A. (2018). The importance of local settings: within-year variability in seawater temperature at South Bay, Western Antarctic Peninsula. PeerJ 6:e4289 https://doi.org/10.7717/peerj.4289

Carrasco, J.F., Bozkurt, D., & Cordero, R.R. (2021). A review of the observed air temperature in the Antarctic Peninsula. Did the warming trend come back after the early 21st hiatus?. Polar Science. https://doi.org/10.1016/j.polar.2021.100653

Chang, K., Jun, H.K., Park, G., & Eo, Y. (1990). Oceanographic Conditions of Maxwell Bay, King George Island, Antarctica (Austral Summer 1989). Korean Journal of Polar Research 1, 27-46

658 Clem, K. R., Renwick, J. A., McGregor, J., & Fogt, R. L. (2016). The relative influence of ENSO
659 and SAM on antarctic Peninsula climate. Journal of Geophysical Research, 121 (16), 9324–9341.
660 doi: 10.1002/2016JD025305607
661
662 Cleveland, R.B., Cleveland, W.S., McRae, J. E., & Terpenning, I. (1990). STL: A seasonal-trend
663 decomposition procedure based on LOESS. Journal of Official Statistics, 6(1), 3-73.
664
665 Coggins, J. H., & McDonald, A. J. (2015). The influence of the Amundsen Sea Low on the winds
666 in the Ross Sea and surroundings: Insights from a synoptic climatology. Journal of Geophysical
667 Research, 120 (6), 2167–2189. doi: 10.1002/2014JD022830
668
669 Costa, D. P., Klinck, J. M., Hofmann, E. E., Dinniman, M. S., & Burns, J. M. (2008). Upper ocean
670 variability in west Antarctic Peninsula continental shelf waters as measured using instrumented
671 seals. Deep-Sea Research Part II: Topical Studies in Oceanography, 55 (3-4), 323–337. doi:
672 10.1016/j.dsr2.2007.11.003614
673
674 Doddridge, E. W., & Marshall, J. (2017). Modulation of the Seasonal Cycle of Antarctic Sea Ice
675 Extent Related to the Southern Annular Mode. Geophysical Research Letters, 44 (19), 9761–9768.
676 doi: 10.1002/2017GL074319
677
678 Donlon, C.J., Martin, M., Stark, J., Roberts-Jones, J., Fiedler, E., & Wimmer, W. (2012). The
679 Operational Sea Surface Temperature and Sea Ice Analysis (OSTIA) system. Remote Sens.
680 Environ., 116, 140–158.
681
682 Fairall, C. W., Bradley, E. F., Hare, J., Grachev, A. A., & Edson, J. B. (2003). Bulk parameterization
683 of air–sea fluxes: Updates and verification for the coare algorithm. Journal of climate, 16 (4), 571–
684 591.
685
686 Gill, A. E. (1982). Atmosphere-Ocean dynamics. Academic Press, New York Elsevier Eds 662 pp.
687

Good, S., Fiedler, E., Mao, C., Martin, M. J., Maycock, A., Reid, R., Roberts-Jones, J., Searle, T., Waters, J., While, J., & et al. (2020). The Current Configuration of the OSTIA System for Operational Production of Foundation Sea Surface Temperature and Ice Concentration Analyses. Remote Sensing 12, no. 4: 720. https://doi.org/10.3390/rs12040720

Global Monitoring and Forecasting Center. (2023). Global Ocean 1/12° Physics Analysis and Forecast updated Daily, E.U. Copernicus Marine Service Information. Retrieved from https://www.copernicus.eu/en/access-data/copernicus-services624-catalogue/global-ocean-112deg-physics-analysis-and-forecast-updated

González-Herrero, S., Barriopedro, D., Trigo, R. M., López-Bustins, J. A., & Oliva, M. (2022). Climate warming amplified the 2020 record-breaking heatwave in the Antarctic Peninsula. Communications Earth & Environment, 3 (1), 122. https://doi.org/10.1038/s43247-022-00450-5

Goyal, R., Jucker, M., Sen Gupta, A., & England, M. H. (2021). Generation of the Amundsen Sea Low by Antarctic orography. Geophysical Research Letters, 48, e2020GL091487. https://doi.org/10.1029/

Hall, A., & Visbeck, M. (2002). Synchronous Variability in the Southern Hemisphere Atmosphere, Sea Ice, and Ocean Resulting from the Annular Mode *. Journal of Climate, 15 (21), 3043–3057.631

Hastie, T., & Tibshirani, R. (1986). Generalized Additive Models. Statistical Science, 1 (3), 297–318. Retrieved from https://projecteuclid.org/download/pdf 1/euclid.ss/1177013437

Hobday, A. J., Alexander, L. V., Perkins, S. E., Smale, D. A., Straub, S. C., Oliver, E. C., & et al (2016). A hierarchical approach to defining marine heatwaves. Progress in Oceanography, 141 , 227–238.

Höfer, J., Giesecke, R., Hopwood, M. J., Carrera, V., Alarcón, E., & González, H. E. (2019). The role of water column stability and wind mixing in the production/export dynamics of two bays in

719 the Western Antarctic Peninsula. Progress in Oceanography, 174 , 105–116. doi:
720 10.1016/j.pocean.2019.01.005
721
722 Holbrook, N. J., Scannell, H. A., Sen Gupta, A., Benthuysen, J. A., Feng, M., Oliver, E. C., & et
723 al. (2019). A global assessment of marine heatwaves and their drivers. Nature communications, 10
724 (1), 2
725
726 Hosking, J. S., Orr, A., Bracegirdle, T. J., & Turner, J. (2016). Future circulation changes off West
727 Antarctica: Sensitivity of the Amundsen Sea Low to projected anthropogenic forcing. Geophysical
728 Research Letters, 43 (1), 367–376. doi: 10.1002/2015GL067143
729
730 Hosking, J. S., Orr, A., Marshall, G. J., Turner, J., & Phillips, T. (2013). The influence of the
731 Amundsen-bellingshausen seas low on the climate of West Antarctica and its representation in
732 coupled climate model simulations. Journal of Climate, 26 (17), 6633–6648. doi: 10.1175/JCLI-
733 D-12-00813.1
734
735 Iriarte, J., Gómez, I., González, H., Nahuelhual, L., & Navarro, J. (2019). Subantarctic and
736 Antarctic Marine Ecosystems: outlining patterns and processes in a changing ocean. Progress in
737 Oceanography, 174 , 1–6.
738
739 Iskandar, M.R, Ismail, MFA., Arifin, T., & Chandra, H. (2021). Marine heatwaves of sea surface
740 temperature off south Java. Heliyon(7): 12,https://doi.org/10.1016/j.heliyon.2021.e08618.
741
742 Latorre, M.P., Iachetti, C.M., Schloss, I.R., Antoni, J., Malits, A., de la Rosa F., De Troch M.,
743 Garcia, M.D., Flores-Melo X., Romero S.I., Gil M.N., & Hernando, M. (2023). Summer heatwaves
744 affect coastal Antarctic plankton metabolism and community structure. Journal of Experimental
745 Marine Biology and Ecology. https://doi.org/10.1016/j.jembe.2023.151926
746
747 Lefebvre, W., Goosse, H., Timmermann, R., & Fichefet, T. (2004). Influence of the Southern
748 Annular Mode on the sea ice - Ocean system. Journal of Geophysical Research C: Oceans, 109
749 (9), 1–12. doi: 10.1029/2004JC002403

Li, Z., Wan, L., Liu, Y., Wang, Z., & Wu, L. (2023). Analysis of Marine Heatwaves in China's Coastal Seas and Adjacent Offshore Waters. Atmosphere 14,1738. https://doi.org/10.3390/atmos14121738

Llanillo, P. J., Aiken, C. M., Cordero, R. R., Damiani, A., Sepúlveda, E., & Fernández-Gómez, B. (2019). Oceanographic Variability induced by Tides, the Intraseasonal cycle and warm subsurface water intrusions in Maxwell Bay, King George Island (West-Antarctica). Scientific Reports, 9 (1). doi: 10.1038/s41598-019-54875-8

Loeb, V., Hofmann, E. E., Klinck, J. M., & Holm-Hansen, O. (2010). Hydrographic control of the marine ecosystem in the South Shetland-Elephant Island and Bransfield Strait region. Deep-Sea Research Part II: Topical Studies in Oceanography, 57 (7-8), 519–542. doi: 10.1016/j.dsr2.2009.10.004

Marshall, G. J. (2003). Trends in the Southern Annular Mode from Observations and Reanalyses. Journal of Climate, 16 , 4134–4143.

Marshall, G. J. (2007). Half-century seasonal relationships between the Southern Annular Mode and Antarctic temperatures. International Journal of Climatology, 27 (3), 373–383. doi: 10.1002/joc.1407

Marshall, G. J. (2020). An observation-based SAM index. Retrieved from https://legacy.bas.ac.uk/met/gjma/sam.html

Maykut, G., & Church, P. (1973). Radiation climate of Barrow, Alaska, 1962-66. Journal of Applied Meteorology, 12 , 620–638.

Meredith, M. P., Falk, U., Bers, A.V., Mackensen, A., Schloss, I.R., Ruiz Barlett, E., Jerosch, K., Silva Busso, A., & Abele, D. (2018). Anatomy of a glacial meltwater discharge event in an

780 Antarctic cove. Philosophical Transactions of the Royal Society A: Mathematical, Physical and
781 Engineering Sciences 376, 20170163. https://doi.org/10.1098/rsta.2017.0163
782
783 Montie, S., Thomsen, M.S., Rack, W., Broady, P.A. (2020). Extreme summer marine heatwaves
784 increase chlorophyll a in the Southern Ocean. Antarct. Sci. 32 (6), 508–509.
785 https://doi.org/10.1017/S0954102020000401.
786
787 Parkinson, C. L., & Washington, W. M. (1979). A Large-Scale Numerical Model of Sea Ice Work
788 at the National Center for Atmospheric (Vol. 84; Tech. Rep.).
789
790 Pawlowicz, R. (2020). M Map: A mapping package for MATLAB. Retrieved from
791 https://www.eoas.ubc.ca/~rich/map.html
792
793 Raphael, M. N. (2004). A zonal wave 3 index for the Southern Hemisphere. Geophysical Research
794 Letters, 31 (23), 1–4. doi: 10.1029/2004GL020365684
795
796 Raphael, M. N., Marshall, G. J., Turner, J., Fogt, R. L., Schneider, D., Dixon, D. A., & Hobbs, W.
797 R. (2016). The Amundsen sea low: Variability, change, and impact on Antarctic climate. Bulletin
798 of the American Meteorological Society, 97 (1), 111–121. doi: 10.1175/BAMS-D-14-00018.1688
799
800 Reda, I., & Andreas, A. (2008). Solar Position Algorithm for Solar Radiation Applications (Tech.
801 Rep.). National Renewable Energy Laboratory.
802
803 Reynolds, R. W., Smith, T. M., Liu, C., Chelton, D. B., Casey, K. S., & Schlax, M. G. (2007). Daily
804 high-resolution-blended analyses for sea surface temperature. Journal of Climate, 20 (22), 5473–
805 5496. doi: 10.1175/2007JCLI1824.1
806
807 Robinson, S. A., Klekociuk, A. R., King, D. H., Pizarro Rojas, M., Zúñiga, G. E., & Bergstrom,
808 D. M. (2020). The 2019/2020 summer of Antarctic heatwaves (Vol. 26)(No. 6). Blackwell
809 Publishing Ltd. doi: 10.1111/gcb.15083
810

Rosselló P., Pascual A. & Combes V. (2023). Assessing marine heat waves in the Mediterranean Sea: a comparison of fixed and moving baseline methods. Front. Mar. Sci. 10:1168368. doi: 10.3389/fmars.2023.1168368

Ruiz Barlett, E.M., Sierra, M.E., Costa A.J., & Tosonotto, G.V. (2021). Interannual variability of hydrographic properties in Potter Cove during summers between 2010 and 2017. Antarctic Science. doi:10.1017/S0954102020000668

Sangrà, P., Gordo, C., Hernández-Arencibia, M., Marrero-Díaz, A., Rodríguez-Santana, A., Stegner, A., Martínez-Marrero, A., Pelegrí, J.L., & Pichon T. (2011). The Bransfield current system. Deep-Sea Research Part I: Oceanographic Research Papers, 58 (4), 390–402. doi: 10.1016/j.dsr.2011.01.011

Sato, K., Inoue, J., Simmonds, I., & Rudeva, I. (2021). Antarctic Peninsula warm winters influenced by tasman sea temperatures. nature communications, 12 (1), 1497.

Schloss, I. R., Abele, D., Moreau, S., Demers, S., Bers, A. V., González, O., & Ferreyra, G. A. (2012). Response of phytoplankton dynamics to 19-year (1991-2009) climate trends in Potter Cove (Antarctica). Journal of Marine Systems, 92 (1), 53–66. doi:10.1016/j.jmarsys.2011.10.006706

Schlosser, E., Alexander Haumann, F., & Raphael, M. N. (2018). Atmospheric influences on the anomalous 2016 Antarctic sea ice decay. Cryosphere, 12 (3), 1103–1119. doi:10.5194/tc-12-1103-2018

Siegert M.J., Bentley M.J., Atkinson A., Bracegirdle T.J., Convey P., Davies B., Downie R., Hogg A.E., Holmes C., Hughes K.A., Meredith M.P., Ross N., Rumble J. & Wilkinson J. (2023). Antarctic extreme events. Frontiers in Environmental Science 11:1229283. doi: 10.3389/fenvs.2023.1229283

Simpkins, G. R., Ciasto, L. M., Thompson, D. W., & England, M. H. (2012). Seasonal relationships between large-scale climate variability and antarctic sea ice concentration. Journal of Climate, 25 (16), 5451–5469. doi: 10.1175/JCLI-D-11-00367.1

Smith, & Klinck. (2002). Water properties on the west Antarctic Peninsula continental shelf: a model study of effects of surface fluxes and sea ice. Deep-Sea Research II , 49 , 4863–4886.715

Smith, R., Baker, K. S., Fraser, W. R., Hofmann, E. E., Karl, D. M., Klinck, J. M., Vernet, M. (1995). The Palmer LTER: A long-term ecological research program at Palmer Station, Antarctica. Oceanography, 8 (3), 77–86. Retrieved from http://www.jstor.org/stable/43924713719

Song S-Y, Kim Y-J, Lee E-J, Yeh S-W, Park J-H and Park Y-G (2023) Wintertime sea surface temperature variability modulated by Arctic Oscillation in the northwestern part of the East/Japan Sea and its relationship with marine heatwaves. Frontiers of Marine Science 10:1198418. doi: 10.3389/fmars.2023.1198418

Stuecker, M. F., Bitz, C. M., & Armour, K. C. (2017). Conditions leading to the unprecedented low Antarctic sea ice extent during the 2016 austral spring season. Geophysical Research Letters, 44 (17), 9008–9019. doi: 10.1002/2017GL074691.

Sun, D., Li, F., Jing, Z. (2023). Frequent marine heatwaves hidden below the surface of the global ocean. Nature Geoscience. 16, 1099–1104. https://doi.org/10.1038/s41561-023-01325-w

The Copernicus Climate Change Service. (2023). Climate bulletins. Retrieved from https://climate.copernicus.eu/sea-ice

Thompson, D. W. J., Wallace, J. M., & Hegerl, G. C. (2000). Annular Modes in the Extratropical Circulation. Part II: Trends*. Journal of Climate, 13 (5), 1018–1036.

Turner, J., Colwell, S., & Harangozo, S. (1997). Variability of precipitation over the coastal western Antarctic Peninsula from synoptic observations. Journal of Geophysical Research Atmospheres, 102 (D12), 13999–14007. doi: 10.1029/96JD03359

Turner, J., Phillips, T., Hosking, J. S., Marshall, G. J., & Orr, A. (2013, 6). The Amundsen Sea Low. International Journal of Climatology, 33 (7), 1818–1829. doi: 10.1002/joc.3558732

Valdivia, N., Garrido, I., Bruning, P., Piñones, A., & Pardo, L. M. (2020). Biodiversity of an antarctic rocky subtidal community and its relationship with glacier meltdown processes. Marine Environmental Research, 159 , 104991.

Yoo, K. C., Lee, M. K., Yoon, H. I., Lee, Y. I., & Kang, C. Y. (2015). Hydrography of Marian Cove, King George Island, West Antarctica: Implications for ice-proximal sedimentation during summer. Antarctic Science, 27 (2), 185–196. doi: 10.1017/S095410201400056X

Yuan, X., & Li, C. (2008). Climate modes in southern high latitudes and their impacts on Antarctic sea ice. Journal of Geophysical Research: Oceans, 113 (6). doi: 10.1029/2006JC004067742

Yuan, X., & Martinson, D. G. (2000). Antarctic Sea Ice Extent Variability and Its Global Connectivity. Journal of Climate, 13, 1697–1717, https://doi.org/10.1175/1520-0442(2000)013<1697:ASIEVA>2.0.CO;2.

Yuan, X., & Martinson, D. G. (2001). The Antarctic dipole and its predictability. Geophysical Research Letters, 28 (18), 3609–3612. doi: 10.1029/2001GL012969